ADVANCED FUNCTIONAL MATERIALS
www.afm-journal.de



# Electron Holography Studies on Narrow Magnetic Domain Walls Observed in a Heusler Alloy $Ni_{50}Mn_{25}Al_{12.5}Ga_{12.5}$

*Hyun Soon Park,* Yasukazu Murakami, Keiichi Yanagisawa, Tsuyoshi Matsuda, Ryosuke Kainuma, Daisuke Shindo, and Akira Tonomura*

**Peculiar magnetic domain walls produced in Heusler alloys, which have attracted renewed interest due to their potential application to actuators and spintronic devices, are studied here using electron holography. The observations reveal unexpectedly narrow magnetic domain walls, the width of which showed perfect agreement with that of the antiphase boundaries (APB, e.g., only 3 nm). While the results can be explained by the significant depression of ferromagnetism due to the local chemical disorder, the electron phase shift indicates that ferromagnetic correlation still remains in the APB region.**

## 1. Introduction

Heusler alloys, which show the $L2_1$-type ordered structure, have been attracting increasing attention due to their enriched functionalities related to spintronics (as a source of spin-polarized current), thermoelectric elements, magnetic refrigeration, etc.[1–4] A giant magnetostriction, which is observed in several magnetic shape memory alloys (SMAs), is another important function provided by Heusler alloys.[5–7] A $Ni_{50}Mn_{25}Al_{12.5}Ga_{12.5}$ alloy is one such system belonging to the group of magnetic SMAs.[8]

Dr. H. S. Park, Prof. Y. Murakami, Prof. D. Shindo, Prof. A. Tonomura
Advanced Science Institute
RIKEN, Wako, Saitama 351-0198, Japan
E-mail: hspark@riken.jp
Prof. Y. Murakami, Prof. D. Shindo
Institute of Multidisciplinary Research for Advanced Materials
Tohoku University
Sendai, Miyagi 980-8577, Japan
K. Yanagisawa, Prof. A. Tonomura
Okinawa Institute of Science and Technology Graduate University
Onna-son, Okinawa 904-0495, Japan
Dr. T. Matsuda
Japan Science and Technology Agency
Kawaguchi-shi, Saitama 332-0012, Japan
Prof. R. Kainuma
Department of Materials Science
Graduate School of Engineering
Tohoku University, Sendai, Miyagi 980-8579, Japan
Prof. A. Tonomura
Central Research Laboratory
Hitachi, Ltd., Hatoyama, Saitama 350-0395, Japan

DOI: 10.1002/adfm.201103052

With respect to the research and/or application of magnetic SMAs, one of the most important factors is the effect of structural imperfections and/or chemical disordering on the magnetic properties. Researchers are particularly interested in the strong interaction between the magnetic domain wall (DW) and antiphase boundary (APB: a planar defect in which the $L2_1$-type order is locally depressed) in Heusler alloys.[9,10] Some of the authors[10] carried out Lorentz microscopy studies that revealed an unexpectedly narrow 180° DW located at the position of APB: *e.g.*, the observed width (12 nm) was considerably less than that (48 nm) for a 180° wall in the matrix region. To gain a deeper understanding of the nature of this narrow DW, we need to measure the width of the APB in the same position as that used for magnetic imaging. However, a critical examination of such nm-scale walls/boundaries has not been completed due to the resolution limit of magnetic imaging and other such technical problems. This motivated us to perform electron microscopy observations of such walls/boundaries with high precision.

Among the magnetic imaging techniques, magnetic force microscopy has a lateral resolution of approximately 20 nm,[11] which is insufficient for observing narrow DWs. With Lorentz microscopy, the Foucault (in-focus) mode of observation has a spatial resolution of 5 nm.[12] However, it is difficult to determine the magnetization distribution in the neighborhood of an APB by using the Foucault method. Our methodology of choice was therefore electron holography,[13] as it enabled us to observe the in-plane magnetic flux component with sufficient lateral resolution (less than 5 nm). We used it to determine the magnetization distribution in the vicinity of an APB in a $Ni_{50}Mn_{25}Al_{12.5}Ga_{12.5}$ alloy.

## 2. Results and Discussion

The dark-field image in **Figure 1**a reveals the APB positions, several of which are indicated by bright lines. Within the framework of a classical thermodynamical theory,[14] the free energy of the system ($F$) in the presence of fluctuations of the order parameter $\eta$ can be expressed as Equation 1:

$$F(\eta) = \int \{f(\eta) + \kappa(\nabla\eta)^2\} \mathrm{d}V, \quad (1)$$

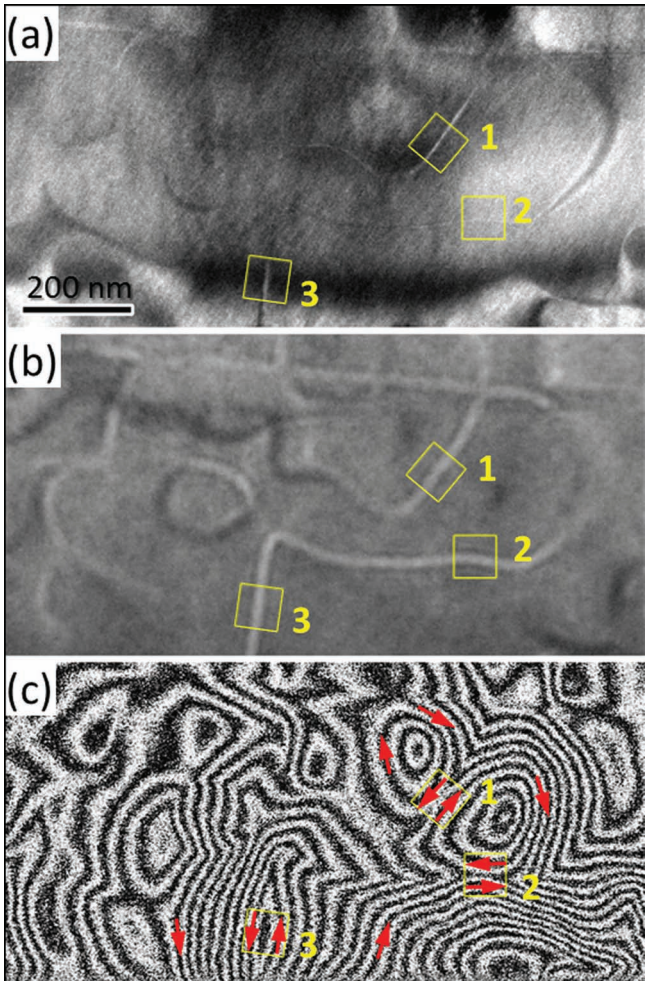


**Figure 1.** Correspondence of the antiphase boundary (APB) and 180° domain wall (DW). a) Dark-field image showing representative APBs. b) DWs imaged using the Fresnel method of Lorentz microscopy. DWs appear as white and black lines. c) Reconstructed phase image showing the magnetic flux distribution. 180° DWs are visible at positions 1–3, as indicated with yellow boxes.

where $f(\eta)$ stands for the free energy per unit volume, $\kappa$ is a constant, $\nabla$ represents the gradient, and the integral should be carried out for the entire volume $V$. An essential point is that the system favors a gradual change in the order parameter due to the second term, $\kappa(\nabla\eta)^2$. If $\eta$ is assumed to represent the degree of chemical order in the $L2_1$-type structure, Equation 1 predicts a finite width APB in which $\eta$ gradually changes. For evaluating the APB width, we chose several points at which the broadness of the APB contrast was minimized: refer to the positions 1-3 in Figure 1a, at which the tilting of the APB (with respect to the incident electrons) must be minimized. The width was determined from the intensity profile observed for a line across the APB: refer to **Figure 2**b, which shows the result for position 2. The measured APB and DW widths for four points are listed in **Table 1**. A dark-field image of position 4 is shown in the inset of **Figure 3**a. The results in the table are on the order of nm although those for position 3 are an exception. A source of this deviation appears to be the tilting of the APB with respect to the incident electrons.

The Lorentz microscopy image shown in Figure 1b demonstrates that many of the magnetic DWs, which are imaged as bright and/or dark lines, are located in the APB positions. Figure 1c is an electron holography result revealing the in-plane component of the magnetic flux in this viewing field: *i.e.*, the black lines represent the lines of magnetic flux, and the red arrows indicate their directions. This flux map reveals that the DWs showed a pattern of 180° DWs at positions 1-3.

We consider next the width of DWs using the result of electron holography for position 2 in Figure 2a. The area in yellow indicates the region for which the dark-field image shows the contrast of the APB. A typical 180° DW pattern is marked by the red rectangle, in which the direction of magnetic flux is reversed. The upper panel in Figure 2c plots the electron phase shift observed for a line crossing this 180° DW. This plot shows the average for eight observations acquired for the rectangular area in Figure 2a. The slope changes from negative (due to down-spin area in the left region) to positive (due to up-spin in the right area) in the vicinity of the DW. The first derivative of the phase shift, shown in the lower panel in Figure 2c, is related to the distribution of the in-plane component of the magnetic flux $M(x)$. Assuming that the sample thickness (approximately 70 nm) was uniform for this field of view, the in-plane magnetic flux component observed in a conventional 180° DW can be approximated by Equation 2:[15,16]

$$M(x) = c\tanh\left(\frac{x}{\delta}\right), \tag{2}$$

where $\delta$ stands for the magnetic exchange length, $x$ indicates a particular position, and $c$ is a constant. A curve fitting (the red line in Figure 2c) determines the width of the DW ($= \pi\delta$) at 5 ± 2 nm for position 2. The observed DW widths determined using this method are listed in Table 1. Note that all the observations are in prefect agreement with the width of the APB. To the best of our knowledge, this is the first observation that demonstrates perfect agreement between the APB width and DW width.

Here we discuss the magnetism within the narrow APB region. With respect to the specimen we observed, the Mn moment appears to have been significantly larger than the Ni moment.[17] Thus, we focus only on the Mn moment in the following discussion. As mentioned elsewhere,[18–20] the magnetic characteristic in $Ni_2MnX$ Heusler alloys ($X$ = Ga, In, Sb, *etc.*) is a counterbalance between the ferromagnetic and antiferromagnetic spin orders. The Mn-Mn pair favors ferromagnetic coupling when both atoms are located at their regular sites in the $L2_1$-ordered structure. In the disordered state, in which Mn atoms are at irregular sites $X$, the magnetic interaction is antiferromagnetic for nearest neighbor Mn-Mn atoms, with one located at a regular Mn site and one at an irregular site. Thus, we expect a gradual change in the magnetization in the APB region, reflecting a gradual change in the $L2_1$-type ordering.

Figure 3a shows the electron phase shift observed for a line across the extremely narrow APB shown in the inset: the width was only 3 nm, as shown in Table 1. Note that the phase shift in Figure 3a represents only the magnetic information (due to magnetic vector potential $\varphi_M$): *i.e.*, undesired signals due to the mean inner potential (*viz*, the effect of thickness variation) has

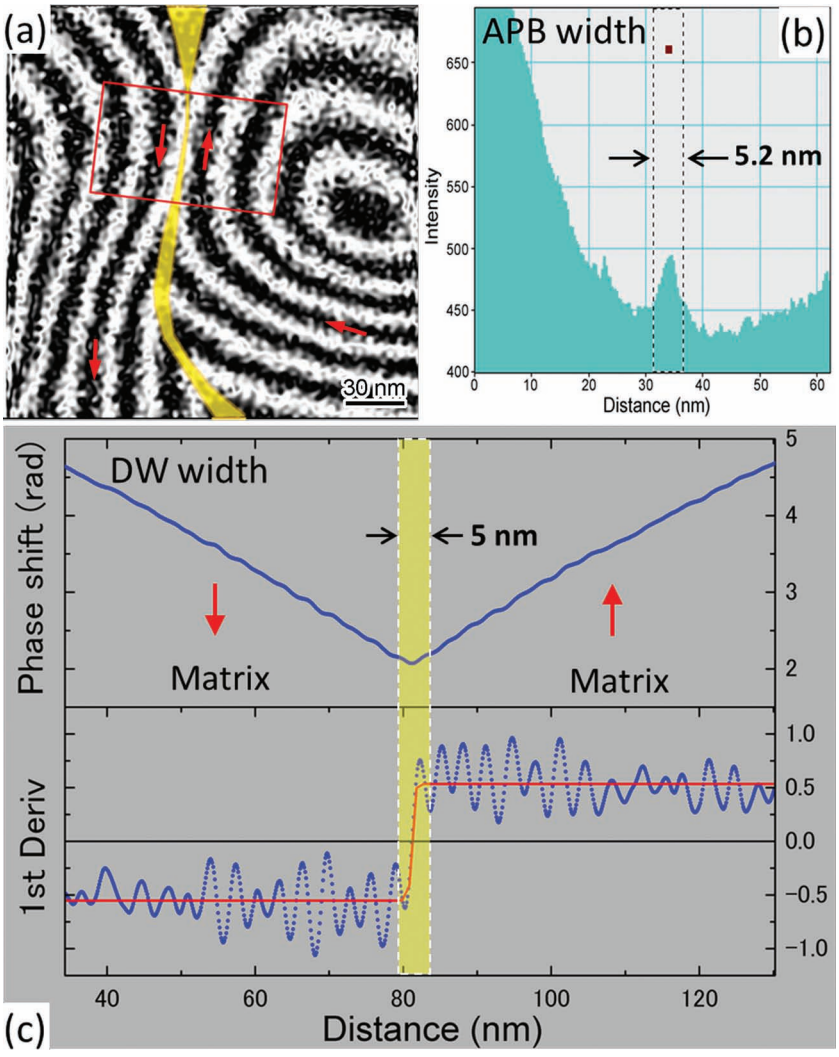


**Figure 2.** Thickness determination of magnetic DW and APB. a) Reconstructed phase image observed for position 2 in Figure 1. Red arrows indicate the direction of magnetic flux. b) Intensity profile measured for a line across APB (at position 2) shown in dark-field image of Figure 1a. c) Phase-shift profile observed for the area indicated by the rectangle in (a). For better phase resolution, the profile was produced by averaging eight unwrapped phase images consecutively acquired under the same exposure conditions.

been eliminated by subtracting one observation representing the original magnetization distribution from one representing magnetization reversal.[13] In an extreme case in which the ferromagnetic order is totally lost in the APB region, the gradient of the curve should be zero over the region APB. However, the observation clearly showed a gradual change in the slope even for this narrow APB. This result indicates that the ferromagnetic coupling still remains within the APB region although the net magnetization must be reduced compared to that of the matrix region due to the chemical disorder.

A challenging study would be to investigate the spin arrangement within the APB region, in which the two types of magnetic correlations are competing. Although this is an extremely difficult condition to address, our electron holography observations may provide useful information for clarifying this complicated behavior. As mentioned above, the plot of the phase shift shows a gradual change in the slope over the region APB: *i.e.*, the narrow DW may have a gradual spin rotation mode similar to that of the conventional 180° DW. Assuming that the lattice parameter of the stoichiometric $Ni_{50}Mn_{25}Al_{12.5}Ga_{12.5}$ alloy is 0.582 nm, we evaluate the atomic distance of the Mn-Mn pair relevant to the ferromagnetic coupling (*i.e.*, Mn atoms located at regular Mn sites) at approximately 0.4 nm. When we consider a simple model with gradual spin rotation, as illustrated in Figure 3b, our observation of the wall width (3 nm) indicates a significant spin rotation angle, 25°, with reference to the distance of these Mn atoms. Surprisingly, this is greater than the rotation angles observed in permanent magnets (*e.g.*, from 5° to 10°), which have nm-scale magnetic DWs due to their large magnetocrystalline anisotropy. We ascribe the significant rotation angle observed for $Ni_{50}Mn_{25}Al_{12.5}Ga_{12.5}$ alloy to a reduction in the effective exchange stiffness. As Lorentz microscopy studies have shown,[10] the exchange stiffness constant for the APB region can be reduced by one order of magnitude (or more) compared with the result for the matrix region when the change in the magnetocrystalline anisotropy is disregarded: the magnetocrystalline anisotropy is initially small in cubic Heusler alloys. To obtain a deeper understanding of the peculiar magnetism in the APB region, we intend to carry out direct measurements of the net magnetization using the holography technique and report the results elsewhere.

**Table 1.** Measured APB and DW widths.

| Position | APB width | 180° DW width |
|---|---|---|
| 1 | 8 nm | 8 nm |
| 2 | 5 nm | 5 nm |
| 3 | 13 nm | 13 nm |
| 4 | 3 nm | 3 nm |

## 3. Conclusion

The sophisticated technique of electron holography has provided essential information for understanding nm-scale magnetic DWs produced in the APB region. The widths of magnetic DWs observed at four different points showed perfect agreement with the APB widths measured at the corresponding positions. These observations unambiguously demonstrate that the unexpectedly narrow DWs are due to the depression

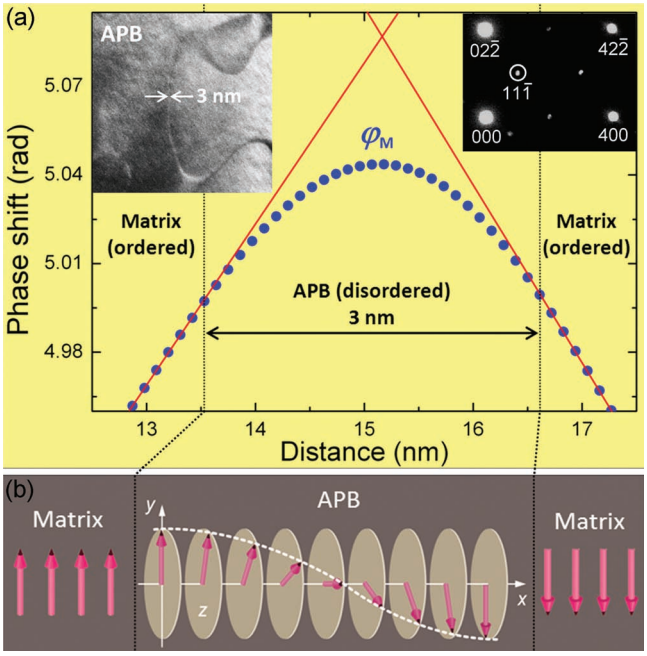


**Figure 3.** Features of the 180° DW at APB position. a) Plot of the electron phase shift due to only the magnetic vector potential $\phi_M$. Gradual deviation from straight red lines (least squares fittings to observations in matrix regions) is clearly seen within the APB. Insets show an electron diffraction pattern of a $Ni_{50}Mn_{25}Al_{12.5}Ga_{12.5}$ alloy with [011] incidence (right) and a dark-field image of 3 nm APB obtained by using the superlattice reflection indicated by white circle in the diffraction pattern (left). b) Schematic illustration showing the gradual spin rotation that may occur in the APB region.

of chemical ordering that occurs within the APB region. The plot of the phase shift showed a gradual change in the slope within the APB region, indicating that a ferromagnetic correlation survives in the APB region, although the interaction is substantially depressed compared with the matrix region. Our observations provide beneficial information for obtaining a deeper understanding of the magnetic order in the vicinity of an interface, which is a core problem not only for ferromagnetic actuators (such as those of magnetic shape memory alloys) but also for spintronic devices.

## 4. Experimental Section

The phase transformations observed in the $Ni_{50}Mn_{25}Al_{12.5}Ga_{12.5}$ alloy are described elsewhere.[8] The alloy ingot was homogenized by heat treatment at 1273 K for three days. For subsequent heat treatment, the ingot was slowly cooled from 1073 K to 673 K over one day, followed by quenching in ice water. A thin-film specimen was prepared by electrochemical polishing. Due to small difference in the scattering amplitude between Mn and (Al, Ga) sites, we were unable to determine accurately the degree of $L2_1$ order by using conventional X-ray diffraction. Nevertheless, an electron diffraction pattern clearly shows superlattice reflections related to $L2_1$ order (e.g., 11-1 spot in the inset of Figure 3), which enabled careful observation of dark-field images about APB. Furthermore, Lorentz microscopy images have demonstrated well defined ferromagnetic domains which can be produced only in the $L2_1$ phase (not in the B2 phase) in this alloy system.[8] We thus believe that the $L2_1$ order in the matrix area is sufficiently developed, and this specimen is useful for in-depth studies of APB.

All experiments were performed with a holography electron microscope (HF-3300X, Hitachi) at an acceleration voltage of 300 kV. This microscope has two positions in which the specimen can be placed. Lorentz microscopy images (out-of-focus images[21,22]) and electron holograms of the DWs were obtained in the field-free position while dark-field images of the APBs were obtained in the objective lens position. The residual magnetic field is approximately 0.01 mT in the field-free position. The holograms were recorded with a Gatan CCD camera (4 K × 4 K, 15 µm/pixel), and reconstructed phase images of the holograms were obtained with Fourier transformation. Details of the electron holography can be found elsewhere.[13]

## Acknowledgements

The authors are grateful to Dr. R. Y. Umetsu for useful discussions about the magnetic structure in this system. This research was supported by the grant from the Japan Society for the Promotion of Science (JSPS) through the "Funding Program for World-Leading Innovative R&D on Science and Technology (FIRST Program)," initiated by the Council for Science and Technology Policy (CSTP).

Received: December 16, 2011
Published online: May 8, 2012

[1] K. Inomata, N. Ikeda, N. Tezuka, R. Goto, S. Sugimoto, M. Wojcik, E. Jedryka, *Sci. Technol. Adv. Mater.* **2008**, *9*, 014101.
[2] S. Chadov, X. Qi, J. Kubler, G. H. Fecher, C. Felser, S. C. Zhang, *Nat. Mater.* **2010**, *9*, 541.
[3] L. Manosa, D. González-Alonso, A. Planes, E. Bonnot, M. Barrio, J.-L. Tamarit, S. Aksoy, M. Acet, *Nat. Mater.* **2010**, *9*, 478.
[4] Y. Nishino, S. Deguchi, U. Mizutani, *Phys. Rev. B* **2006**, *74*, 115115.
[5] K. Ullakko, J. K. Huang, C. Kantner, R. C. O`Handley, V. V. Kokorin, *Appl. Phys. Lett.* **1996**, *69*, 1966.
[6] R. Kainuma, Y. Imano, W. Ito, Y. Sutou, H. Morito, S. Okamoto, O. Kitakami, K. Oikawa, A. Fujita, T. Kanomata, K. Ishida, *Nature* **2006**, *439*, 957.
[7] *Advances in magnetic shape memory materials*, (Ed: V. A. Chernenko), Trans. Tech. Publications, Zurich **2011**.
[8] H. Ishikawa, R. Y. Umetsu, K. Kobayashi, A. Fujita, R. Kainuma, K. Ishida, *Acta Mater.* **2008**, *56*, 4789.
[9] S. P. Venkateswaran, N. T. Nuhfer, M. D. Graef, *Acta Mater.* **2007**, *55*, 2621.
[10] Y. Murakami, T. Yano, R. Y. Umetsu, R. Kainuma, D. Shindo, *Scripta Mater.* **2011**, *65*, 895.
[11] T. Shinjo, T. Okuno, R. Hassdorf, K. Shigeto, T. Ono, *Science* **2000**, *289*, 930.
[12] S. A. Majetich, Y. Jin, *Science* **1999**, *284*, 470.
[13] A. Tonomura, *Electron holography*, 2nd ed., Springer-Verlag, Tokyo **1999**.
[14] J. W. Cahn, *Acta Metall.* **1961**, *9*, 795.
[15] A. Hubert, R. Schäfer, *Magnetic domains*, Springer-Verlag, Berlin **2000**.
[16] Y. Murakami, H. Kasai, J. J. Kim, S. Mamishin, D. Shindo, S. Mori, A. Tonomura, *Nat. Nanotechnol.* **2010**, *5*, 37.
[17] E. Sasioglu, L. M. Sandratskii, P. Bruno, *Phys. Rev. B* **2004**, *70*, 024427.
[18] J. Enkovaara, O. Heczko, A. Ayuela, R. M. Nieminen, *Phys. Rev. B* **2003**, *67*, 212405.
[19] V. Sánchez-Alarcos, V. Recarte, J. I. Pérez-Landazábal, C. Gómez-Polo, J. A. Rodríguez-Velamazán, *Acta Mater.* **2012**, *60*, 459.
[20] E. Sasioglu, L. M. Sandratskii, P. Bruno, *Phys. Rev. B* **2008**, *77*, 064417.
[21] M. De Graef, Y. Zhu, *Magnetic imaging and its applications to materials*, Academic Press, San Diego **2001**.
[22] H. S. Park, Y. Murakami, D. Shindo, V. A. Chernenko, T. Kanomata, *Appl. Phys. Lett.* **2003**, *83*, 3752.